

Photocapacitance study of boron-doped chemical-vapor-deposited diamond

R. Zeisel,* C. E. Nebel, and M. Stutzmann

Walter Schottky Institut, TU München, Am Coulombwall, 85748 Garching, Germany

E. Gheeraert and A. Deneuveille

Laboratoire d'Etudes des Propriétés Electroniques des Solides, CNRS, Boîte Postale 166, 38042 Grenoble Cedex 9, France

(Received 23 December 1998; revised manuscript received 1 March 1999)

We discuss capacitance-voltage and optically excited deep-level transient spectroscopy (ODLTS) experiments carried out on boron-doped diamond, homoepitaxially grown by chemical-vapor deposition. ODLTS reveals an acceptor-type defect at 1.28 eV above the valence-band edge with a concentration of $\approx 1 \times 10^{16} \text{ cm}^{-3}$. From the temperature dependence of the ODLTS spectra, a lattice coupling of this electronic defect level is deduced, which is characterized by a Franck-Condon shift of 0.16 eV. [S0163-1829(99)09827-6]

I. INTRODUCTION

The electronic characterization of diamond is a long-lasting story with ups and downs. Due to the extremely high resistivity of intrinsic diamond, only a limited number of experiments could be applied to elucidate the electronic properties of natural and synthetic material, which, because of its extreme qualities, is promising for a variety of device applications. It has been shown—mainly by luminescence and absorption techniques—that a variety of defects are present with well-defined energy levels in the band gap of diamond. However, very little is known about the effects of disorder on energy levels, capture cross sections of defects, thermal broadening, etc. In semiconductors like Si, GaAs, and the wide band-gap semiconductor GaN,^{1,2} this exciting field of semiconductor physics has been explored by deep-level transient spectroscopy (DLTS), optically excited (O)DLTS, and photoconductivity experiments. The application of (O)DLTS to diamond is limited by the resistivity of the layers, which can be, however, reduced significantly by doping with boron. To perform capacitance transient experiments, it is in addition essential to reduce the frequency of the applied test voltage from MHz (standard capacitance meters) to several ten Hz to account for the emission rate of the boron acceptor and the residual resistivity of the layer.

In this paper, we use ODLTS experiments for boron-doped homoepitaxially grown chemical-vapor-deposited (CVD) diamond to explore the energy regime $0.8 \text{ eV} \leq h\nu \leq 2 \text{ eV}$ above the valence band. In this region, the absorption is strongly dominated by the photoionization of the boron acceptor even at boron concentrations as low as $\approx 10^{16} \text{ cm}^{-3}$ (Refs. 3 and 4). Therefore, photoconductivity experiments are unable to explore defects in this energy regime, when their concentration does not exceed the one of the boron acceptors. Due to the ionization of the boron acceptors in the depletion layer of a Schottky contact, however, they cannot mask the absorption of the defects. So ODLTS experiments are a powerful tool to study optical properties of defects.

II. EXPERIMENT

The CVD diamond investigated here has been grown homoepitaxially in a microwave plasma quartz reactor at

820 °C and 30 Torr gas pressure. The gas composition was 100 sccm hydrogen and 4 sccm methane. Diborane was added resulting in a boron to carbon concentration ratio of 10 ppm in the gas phase. A synthetic type Ib substrate was used, whereupon an undoped buffer layer of 1 micron was deposited, before the 3.5 micron-thick boron-doped layer was grown.

In order to remove hydrogen and graphitic layers from the surface, the sample was kept in boiling *aqua regia* for 1 h and exposed to an oxygen microwave plasma for 25 min. For Ohmic contacts we evaporated titanium/platin/gold of thickness 300/170/1500 Å, and annealed the sample at 500 °C in a forming gas atmosphere for 10 min. Square-shaped Schottky contacts ($1 \times 1 \text{ mm}^2$) were realized by evaporation of 1000 Å aluminum. A coplanar contact configuration has been used, where the spacing between the Ohmic and the Schottky contact was 50 microns. The Schottky contact was illuminated through the substrate. This limits the spectral range to $h\nu \leq 2 \text{ eV}$, since the Ib diamond is strongly absorbing for $h\nu > 2.1 \text{ eV}$. For photon energies $h\nu < 2 \text{ eV}$, we found no significant spectral dependence in transmission spectroscopy of a typical type Ib diamond.

A 100-W quartz tungsten halogen lamp in conjunction with a Spex 270M grating monochromator is used as the light source. Appropriate filters were selected to cut off higher orders. Two concave mirrors focused the light on the Schottky contact, to exclude chromatic aberrations. The relative intensity of the incident light was monitored by a pyroelectric detector. The sample was mounted in a continuous flow cryostat. An ac voltage of 100 mV and 84 Hz was applied to the reverse-biased (2 V) diode. The capacitance was calculated from the absolute value of the current and its phase shift relative to the applied voltage. Details of the experimental setup are described elsewhere.⁵

The basic relation used to obtain the ODLTS spectra is

$$\left. \frac{dC(t)}{dt} \right|_{t \approx 0} \sim \sigma_o N_T \phi, \quad (1)$$

where C is the capacitance, t the time, σ_o the photoionization cross section, N_T the defect density of the sample, and ϕ the flux of the incident light. This relation connects the defect

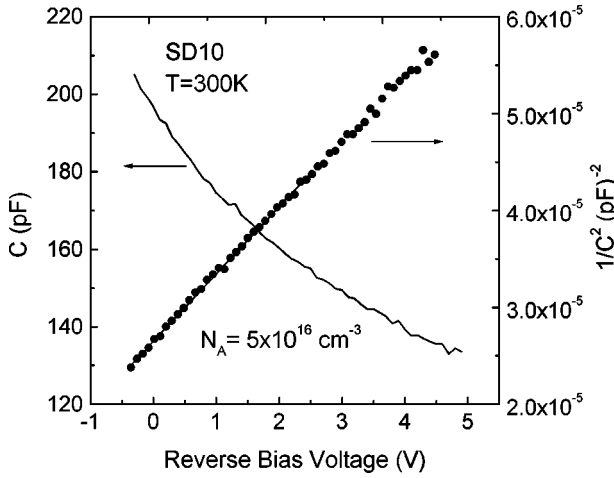


FIG. 1. Capacitance-voltage characteristics at 300 K in the dark (squares). From the slope of a linear fit to the $1/C^2$ data (solid lines), an acceptor density of $5 \times 10^{16} \text{ cm}^{-3}$ was determined.

absorption coefficient $\alpha = \sigma_o N_T$ with the initial slope of the capacitance transients. Plotting these slopes—normalized to the incident photon fluxes—versus the photon energy provides the spectral dependence of the absorption coefficient (Ref. 6). Due to the contact configuration and the experimental setup, the absorption coefficient can be calculated only in relative units.

III. RESULTS AND DISCUSSION

The Schottky contacts give rise to normal diode capacitance-voltage characteristics, which are shown in Fig. 1. The curve was recorded at 300 K in the dark. From the slope in the $1/C^2$ plot we obtain an acceptor density⁷ of $5 \times 10^{16} \text{ cm}^{-3}$.

The ODLTS spectrum at 300 K—obtained from the initial rise of the capacitance transients—is shown in Fig. 2 (squares). A threshold at 1.0 eV is detected. The absorption steeply increases over 4 orders of magnitude and shows a maximum at 1.65 eV. For $h\nu \geq 1.65 \text{ eV}$, the absorption decreases. To determine the trap levels from optical absorption one commonly calculates fits of theoretical photoionization cross sections to the experimental data based on^{8,9}

$$\sigma_o \sim \frac{\varrho(h\nu - E_T)}{h\nu} \frac{(h\nu - E_T)^\delta}{(h\nu)^{2\gamma}}, \quad (2)$$

where E_T is the trap level and $\varrho(E)$ the density of states in the valence band. δ can be 0 or 1, which defines an allowed or a forbidden transition, respectively, and γ , either 0 or 1, stands for an indirect or a direct transition, respectively. However, none of the four theoretical cross sections can be fitted satisfactorily to the experimental data. For example, the best calculated fit of a cross section with trap energy at 1.28 eV, $\varrho(E) \sim E^{1/2}$, $\delta = 1$, and $\gamma = 1$ is shown in the inset of Fig. 2. Although a good agreement between the optical cross section and the experimental data for $h\nu \geq 1.6 \text{ eV}$ is achieved, the deviation below 1.6 eV is obvious, indicating a significant level broadening of the absorption centers.

Broadening can have various causes. It can be due to bonding disorder introduced by structural imperfection such as dislocations in the layer. More important, however, is

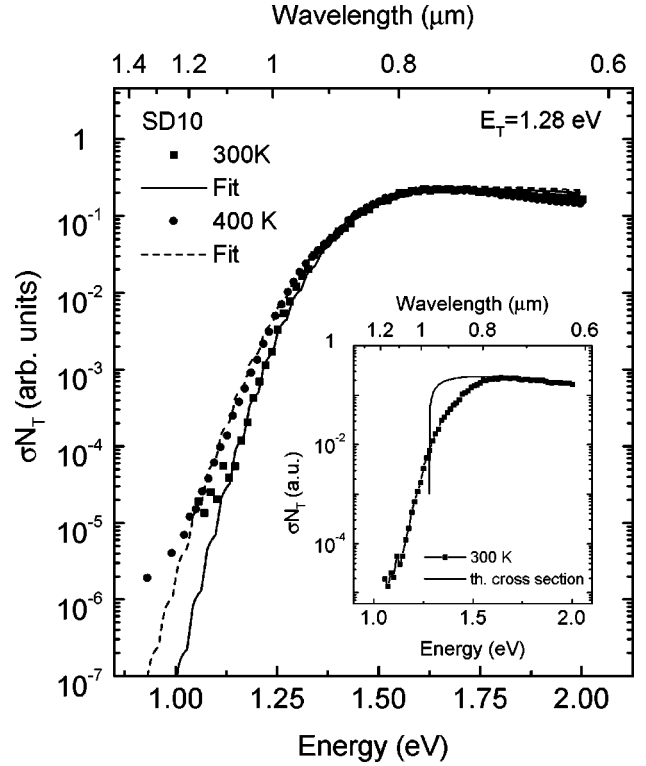


FIG. 2. ODLTS spectra of a boron-doped CVD-diamond at 300 K (squares) and 400 K (circles). Also included are the theoretical calculations for the absorption at the two temperatures after Eq. (7). The inset shows the spectrum at 300 K with a photoionization cross section after Inkson.

thermally induced broadening, which becomes evident by comparing the spectra measured at different temperatures as shown in Fig. 2. The two spectra, recorded at 300 and 400 K, are normalized to $\sigma_o N_T(1.6 \text{ eV})$. For photon energies $h\nu < 1.25 \text{ eV}$ a strong temperature dependence of the absorption can be recognized.

To calculate the energy level of the defect detected by ODLTS, we assume the lattice relaxation model, which manifests itself in a Stokes shift of the transition energy for optical ionization relative to the energy necessary for thermal ionization. This is schematically shown in Fig. 3. Here, the lattice energy plus the electronic energy of the initial (lower parabola) and the final (upper parabola) state is plotted versus the configuration coordinate. After photoionization, the hole is delocalized in the valence band. Therefore, the final state is defined by the vibronic states of the defect and the density of states of the valence band. Accounting for this, the resulting optical cross section σ_o^L has to be recalculated, since the expression for σ_o from Eq. (2) does not include any electron-phonon interaction. Here we follow the approach of Jaros¹⁰

$$\sigma_o^L(h\nu) = \frac{1}{h\nu} \int |\langle \Phi | -i\hbar \vec{\nabla} | \psi_T \rangle|^2 L(\epsilon, h\nu) \varrho(\epsilon) d\epsilon, \quad (3)$$

where Φ and ψ_T are the wave functions of holes in the valence band and in the trap, respectively. As Hamilton operator, the standard dipole approximation of the electromagnetic field is used. $L(\epsilon, h\nu)$ is the line-shape function that takes into account the different transition probabilities between the vibrational states α and β of the defect and has been treated

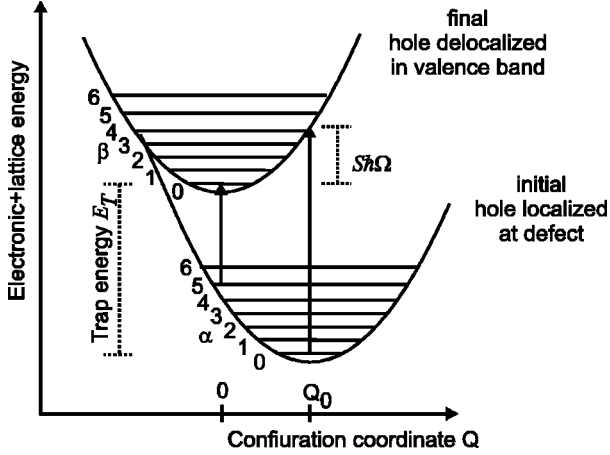


FIG. 3. The configuration coordinate diagram for deep levels. The two parabola—initial and final defect state—with the vibrational defect levels are shifted horizontally by the change in configuration coordinate and vertically by the trap energy E_T . Optical transitions between different vibronic states of initial and final defect state are marked with arrows.

in detail by Keil.¹¹ When the lattice coupling is treated quantum mechanically, L consists of a sum over weighted delta functions, which represent the contribution of each vibrational state of the defect to the photoionization. Most authors replace this sum of delta functions by a Gaussian function. This is valid in the so-called high-temperature/strong coupling limit,¹² which is defined by a large Huang-Rhys factor S and high temperatures, i.e., phonon energy $\hbar\Omega \ll kT$. But these conditions are not fulfilled in many cases, since—especially in diamond—the phonon energies are equal to or even larger than kT in the temperature range considered here. Therefore, we use the full quantum-mechanical expression for the line-shape function

$$L(E, h\nu) = \sum_{p=-\infty}^{\infty} \delta(p\hbar\Omega + E_T + E - h\nu) W(p) \quad (4)$$

where $W(p)$ is the weighting function and is defined by¹¹

$$W(p) = \exp[p\hbar\Omega/2kT - S \coth(\hbar\Omega/2kT)] \times I_p[S \operatorname{cosech}(\hbar\Omega/2kT)]. \quad (5)$$

In these equations I_p is the Bessel function of the first kind with imaginary argument, $\hbar\Omega$ the energy of the involved phonon and $h\nu$ the energy of the incident photons. p is defined by $p = \alpha - \beta$ where α and β are the quantum numbers of the phononic excitation of the ground state and the ionized state of the defect, respectively.

The integral Eq. (3) now decays in a sum over weighted matrix elements

$$\sigma_o^L(h\nu) = \frac{1}{h\nu} \sum_{p=-\infty}^{\infty} W(p) [|\langle \Phi | -i\hbar \nabla | \psi \rangle|^2 \times \varrho(h\nu - E_T - p\hbar\Omega)]. \quad (6)$$

For the calculation of the matrix elements we again rely on the model of Inkson.⁸ Thus, we get, using $\varrho(E) \sim E^{1/2}$

TABLE I. Numerical values of the fit parameters, which have been used to fit the experimental data by a theoretical model.

Parameter		Value
	γ	1
	δ	1
Phonon energy	$\hbar\Omega$	35 meV
Huang-Rhys Factor	S	4.5
Franck-Condon shift	$S\hbar\Omega$	0.16 eV
Trap energy	E_T	1.28 eV

$$\sigma_o^L(h\nu) \sim \frac{1}{h\nu} \sum_p W(p) \frac{(h\nu - E_T - p\hbar\Omega)^{\gamma+1/2}}{(h\nu - p\hbar\Omega)^{2\delta}}, \quad (7)$$

where γ and δ have the same meanings as in Eq. (2).

Equation (7) contains five free parameters of interest, namely the trap energy E_T , the two parameters for the photoionization cross section γ and δ , the Huang-Rhys factor S —present in $W(p)$ —and the phonon energy $\hbar\Omega$. From the presence of a maximum in the measured absorption versus energy followed by a decrease towards higher photon energies ($h\nu > 1.65$ eV), we assume $\gamma = 1$, $\delta = 1$, since this is characteristic for a direct, allowed transition. Nothing is known about the phonon energy $\hbar\Omega$ of the defect. In our calculations, we assumed values in the range 30 to 60 meV, which is reasonable due to the fact that in absorption and luminescence experiments on diamond these values are often detected.¹³ Finally S and E_T have been used as fit parameters. The best fits are shown in Fig. 2, the corresponding fit-parameters are summarized in Table I.

It is worth noting that the Huang-Rhys factor S is not independent of the phonon energy $\hbar\Omega$. Varying the latter in the range 15 meV to 50 meV, the best fits were obtained with values of S that were given through $S = 0.16 \text{ eV}/\hbar\Omega$, with a constant Franck-Condon parameter $d = S\hbar\Omega$ of 0.16 eV. For the optical ionization energy we calculate 1.44 eV, using the relation $E_{\text{opt}} = d + E_T$.

The shoulders in the calculated spectrum result from the summation over the individual photoionization cross sections located at $p\hbar\Omega$ around E_T . The lack of this feature in the experimental data allows two conclusions. First, that the local phonon energy is smaller than about 10 meV. These narrow spaced shoulders cannot be resolved within this experiment. However, such a small phonon energy gives rise to a large Huang-Rhys factor ($S \geq 16$) and therefore to strong electron-phonon coupling.

On the other hand, the defect may couple to broad ranges of phonon energies and therefore no discrete structure would be resolved in the measured spectra. Since it is—within the presented experiment—not possible to extract information about the involved phonon energy, the fitting value should be regarded as an effective frequency. However, the main information about the configurational properties is given through the Frank-Condon parameter of 0.16 eV, which is independent of the phonon energy.

Neglecting retrapping of holes, the defect density has been calculated from¹⁴

$$N_T = 2N_A \frac{\Delta C}{C_{SS}(h\nu_1)}, \quad (8)$$

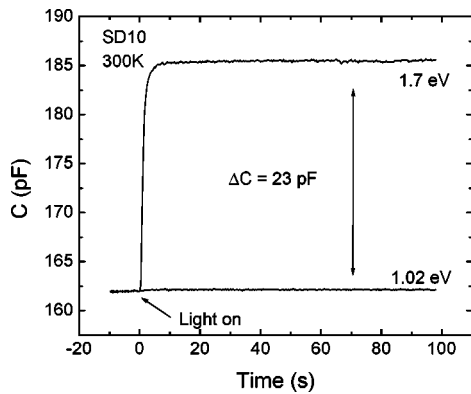


FIG. 4. Two transients capacitances for photon energies $h\nu = 1.02$ eV and 1.7 eV. The change in illuminated steady-state capacitance between the two photon energies is related to the defect density.

where $\Delta C = C_{SS}(h\nu_2) - C_{SS}(h\nu_1)$ is the change of the steady-state capacitance under illumination between two photon energies. This is shown in Fig. 4. $h\nu_1$ has to be lower than the optical ionization energy (here $h\nu_1 = 1.02$ eV) and $h\nu_2$ has to be above the optical ionization energy (here $h\nu_2 = 1.7$ eV). N_A is the acceptor density, which has been calculated from $C-V$ -measurements. For our sample we calculate $N_T \approx 1 \times 10^{16} \text{ cm}^{-3}$ for this level.

Equation (8) is an approximation for $N_T \ll N_A$, which is not fulfilled in our case. Evaluating the exact expression, leads to a slightly lower defect density. However, we consider this as a minor error in comparison with the error introduced by the coplanar contact geometry.

We have observed this defect in various samples from other growth methods and reactors, too. However with different spectral shapes of the absorption due to the superposition of an additional trap.⁵ Even in natural type IIb diamond a defect absorption could be detected at a corresponding energy by Ristein *et al.*¹⁵ The ubiquity of this defect in boron-doped diamonds suggests the relation to a common impurity like nitrogen, an intrinsic defect like a vacancy or a carbon interstitial or even to a boron-induced defect level.

IV. SUMMARY

In this paper, we present ODLTS measurements on boron-doped, homoepitaxially grown CVD diamond. A defect level at 1.28 eV above the valence-band edge with a defect concentration of $\approx 1 \times 10^{16} \text{ cm}^{-3}$ is found. The effect of lattice relaxation after ionization could be demonstrated and revealed a Franck-Condon shift of 0.16 eV. This defect has also been detected in single-crystal synthetic type IIb diamond and other CVD-grown boron-doped layers, which will be published in the near future.

*Electronic address: zeisel@wsi.tu-muenchen.de

- ¹W. Götz, N. M. Johnson, R. A. Street, H. Amano, and I. Akasaki, *Appl. Phys. Lett.* **66**, 1340 (1995).
- ²P. Hacke, H. Miyoshi, K. Hiramatsu, H. Okumura, S. Yoshida, and H. Okushi, and in *III-V Nitrides*, edited by F. A. Ponce, T. D. Moustakas, I. Akasaki, and B. A. Monemar, MRS Symposium Proceedings No. 449 (Materials Research Society, Pittsburgh, 1997), p. 549.
- ³E. Rohrer, C. E. Nebel, M. Stutzmann, A. Flöter, R. Zachai, X. Jiang, and C.-P. Klages, *Diamond Relat. Mater.* **7**, 879 (1998).
- ⁴A. T. Collins, E. C. Lightowers, and P. J. Dean, *Phys. Rev.* **183**, 725 (1969).
- ⁵R. Zeisel, C. E. Nebel, and M. Stutzmann, *J. Appl. Phys.* **84**, 6105 (1998).

- ⁶A. Chantre, G. Vincent, and D. Bois, *Phys. Rev. B* **23**, 5335 (1981).
- ⁷S. M. Sze, *Physics of Semiconductor Devices*, 2nd ed. (Wiley, New York, 1981).
- ⁸J. C. Inkson, *J. Phys. C* **14**, 1093 (1981).
- ⁹H. G. Grimmeis and L.-A. Lebedo, *J. Appl. Phys.* **45**, 2155 (1975).
- ¹⁰M. Jaros, *Phys. Rev. B* **16**, 3694 (1977).
- ¹¹T. H. Keil, *Phys. Rev.* **140**, A601 (1965).
- ¹²M. Lax, *J. Chem. Phys.* **20**, 1752 (1952).
- ¹³*The Properties of Natural and Synthetic Diamond*, edited by J. E. Field (Academic Press, London, 1992).
- ¹⁴D. V. Lang, *J. Appl. Phys.* **45**, 3023 (1974).
- ¹⁵J. Ristein, W. Stein, and L. Ley, *Phys. Rev. Lett.* **78**, 1803 (1997).